




Cite this: *Phys. Chem. Chem. Phys.*,
2017, **19**, 23138

Criticality of the phase transition on stage two in a lattice-gas model of a graphite anode in a lithium-ion battery

E. M. Gavilán Arriazu,^a B. A. López de Mishima,^a O. A. Oviedo,^b E. P. M. Leiva^b and O. A. Pinto *^a

Herein, a Monte Carlo study within the canonical assembly has been applied to elucidate the lithium-ion phase transition order of a stage II lithium–graphite intercalation compound (LiC₁₂) around the critical point. The results reveal a weakly first-order phase transition at 354.6 ± 0.5 K via measurements that follows the power laws with effective exponents. The graphite–lithium system was emulated within a lattice-gas model, comprising specific insertion sites arranged in four parallel planes with a triangular geometry. Moreover, two different types of energetic interactions were used: a Lennard-Jones potential, for particle interactions in the same plane, and a power law potential that decreased with distance, for particles in different planes. The energy per site and order parameter distribution were used to classify the order of the transition. Furthermore, the order parameters, susceptibility, and heat capacity were computed and analyzed.

Received 23rd June 2017,
Accepted 3rd August 2017

DOI: 10.1039/c7cp04253a

rsc.li/pccp

1. Introduction

Lithium-ion batteries have attracted wide interest in current science and technology due to the high demand for energy storage in a large range of electrical products.^{1–3} A high energy density, good cycle life, high operating voltage, and low cost are some of the main characteristics of this type of rechargeable battery. Graphite, a material used as an anode since early 90's, and several cathode materials, including transition metal oxides or phosphates, have been employed as active materials.^{4,5} For this reason, knowing how external variables, such as temperature and pressure, affect the battery materials is crucial to improve their functionality since the changes that produce these variables alter their properties and, hence, the operation of the battery.

The intercalation process of lithium in graphite involve formation of stages, known as lithium–graphite intercalation compounds (LGIC).⁶ The stages are characterized by the periodic structure of the lithium ion layers between graphite sheets and have been analyzed by XRD and electrochemical techniques.^{6–8} The number of graphite sheets between adjacent lithium layers define the stage names. In stage II (LiC₁₂), which has been described in numerous works,^{9–12} there are two graphite layers

between adjacent lithium planes, and the lithium ions follow a specific in-plane ordered structure ($\sqrt{3} \times \sqrt{3}$, $R30^\circ$). Moreover, three types of phase transition may occur during the formation of stage II: (1) an order–disorder phase transition:^{13–19} in this case, the divergences in the thermodynamic functions are associated with the critical exponents (power laws) around the critical point when the correlation function diverges; (2) a first-order phase transition:^{20–27} at the critical point, the ordered and disordered states co-exist; and finally, (3) a first-order phase transition that follows the power laws in the neighborhood of the critical point, also known as weak first-order phase transitions.^{28–30} In this kind of transition, a few effective exponents, each one associated with some thermodynamic function can be observed, similar to the phase transition described in (1).

There are experimental and theoretical studies reported on the phase transition of various graphite intercalation compounds (GIC)^{31–34} and, more specifically, on the LGIC phase transition.^{35–37} Elastic neutron scattering and scanning calorimetry³⁶ and ac calorimetry and neutron diffraction³⁵ show a weak first-order melting of the Li layers in the LGIC stage-one (LiC₆). The latter authors studied the criticality of stage-one for lithium-intercalated graphite and concluded that the phase transition corresponded to a 3D three-state Potts universality class. Stage-one of C₈Cs, CsRb, and C₆Li compounds was examined within the Landau–Ginzburg theory. In all the cases, a first-order transition was identified, and a 3D three-state Potts model was suggested for C₆Li.³⁷ The same authors analyzed the stage-two of other GIC's, and they concluded that all GIC showed a smeared first-order phase transition.³⁴

^a Instituto de Bionanotecnología del NOA (INBIONATEC-CONICET), Universidad Nacional de Santiago de Estero, RN 9 Km 1125 Villa el Zanjón, Santiago del Estero, G4206XCP, Argentina. E-mail: oapinto@uns.edu.ar

^b Instituto de Físicoquímica de Córdoba, Departamento de Química Teórica y Computacional de la Facultad de Ciencias Químicas, Universidad Nacional de Córdoba, Córdoba X5000HUA, Argentina

Monte Carlo (MC) simulations and finite size scaling are the most commonly used techniques to study phase transitions occurring on the surfaces.^{25,38} On the other hand, MC simulations have also been applied to study intercalated substrates.^{39–41} Moreover, kinetic Monte Carlo (kMC) simulations has been used to model silicate oligomerization in solution,⁴² in the formation of silicate oligomers,⁴³ and in interstellar grain chemistry.⁴⁴ With standard MC simulation, the cluster ordering in a two-dimensional lattice model has been studied in.⁴⁵

If the electrochemical operation of a lithium-ion battery has to be mimicked, it is convenient to apply the grand canonical ensemble. In this scheme, the temperature is constant, but the potential of the electrode and the number of Li ions changes. However, to study critical phenomena, it is more appropriate to use the canonical ensemble, where the number of Li ions is constant and the temperature varies around the critical point. Consequently, in the present study, a standard finite size scaling method in the canonical ensemble was used to analyze the criticality of the phase transition involved in the formation of stage II (LiC_{12}) in LGIC.

The study is organized as follows. In Section 2, the lattice-gas model and details of the theoretical model are presented. Section 3 describes the Monte Carlo simulations and finite-size scaling. The order of the phase transition and estimation of the critical temperature are presented in Section 4. Finally, the conclusions are drawn in Section 5.

2. The theoretical model

An idealized anode electrode designed with four graphite planes was used to carry out the Monte Carlo (MC) simulations. This model has been presented and described in detail by Perassi and Leiva.³⁹ The authors employed it to study the intercalation of lithium ions in graphite to calculate intercalation entropy and enthalpy for the stage II to stage I transition. The authors found a good agreement with experimental measurements. With regard to the model, the adsorption sites correspond to the centers of the carbon hexagons in the graphite bulk with AA stacking and are located at the half distance between two graphene layers.^{46–48} This data was used to define the lattice-gas model, where the distance between adjacent planes was $d_1 = 3.35 \text{ \AA}$ and the distance between first nearest neighbors in the same plane was $d_2 = 2.13 \text{ \AA}$, as is indicated in Fig. 1. Fig. 1(a) shows a lateral view of the system. The grey spheres represent the carbon atoms and the white circles correspond to the empty insertion sites (the real lattice-gas). Then, the lattice was formed by the $N = 4L^2$ specific adsorption sites, where L^2 is the number of sites in each plane. L can be considered as the linear dimension (lateral size) of the system.

The total energy of the system, with lithium ions inserted into graphite, is given by the Hamiltonian function:

$$H = \frac{\rho}{2} \sum_{i \neq j}^{N_{xy}} c_i c_j \left[\left(\frac{4.26 \text{ \AA}}{r_{ij}} \right)^{12} - 2 \left(\frac{4.26 \text{ \AA}}{r_{ij}} \right)^6 \right] + \frac{\kappa}{2} \sum_{i \neq j}^{N_z} c_i c_j \left(\frac{1.42 \text{ \AA}}{r_{ij}} \right)^\alpha + \gamma \sum_{i=1}^N c_i \quad (1)$$

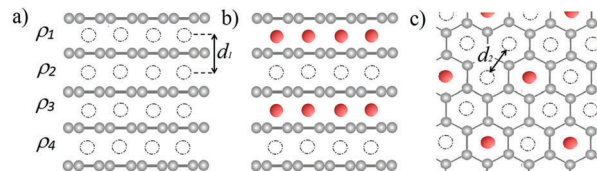


Fig. 1 (a) The lateral scheme of the system. The grey spheres correspond to the carbon atoms and the white circles correspond to the empty adsorption sites. (b) The lateral scheme of stage II. The red spheres correspond to the Li-ions. (c) Top-view of stage II, the Li-ion forms a $(\sqrt{3} \times \sqrt{3})R30^\circ$ structure.

The first sum corresponds to a Lennard-Jones potential and considers the in-plane interactions, *i.e.*, the interactions between the lithium ions placed in the same graphite layer. The second sum corresponds to the repulsive out-plane interactions in this case the lithium ions placed in different graphite layers. The last sum considers the specific lithium-graphite interaction. N_{xy} and N_z correspond to the number of in-plane and out-plane neighbors, respectively. c_i is the usual occupation variable and takes the value 1 if the i site is occupied and 0 otherwise. r_{ij} is the distance between the ij sites in Angstrom units. The factor 1/2 is included due to the double counting links. All the other constants were fitted from the experimental data reported by Perassi and Leiva:³⁹ $\rho = 0.0025 \text{ eV}$ is the attractive interaction value at a distance of 4.26 \AA , $\kappa = 0.025 \text{ eV}$ controls the repulsive interactions, $\alpha = 4$ is a parameter that adjusts the drop of the out-plane interactions, and $\gamma = -0.029 \text{ eV}$ is the energy related to the lithium-graphite interactions.

3. Monte Carlo simulations and finite-size scaling

To study the thermodynamic properties of the Hamiltonian function given in eqn (1), a parallel tempering algorithm or replica Monte Carlo exchange^{30,49–51} was used. This method consists of a system with M -independent replicas, which do not interact between them, each one at a defined temperature. In other words, each i th replica was inserted into a heat bath at a temperature T_i .

The algorithm involves two steps: (i) replica update; vacancy-particle exchange. This means that an ad-particle and an empty site are randomly selected from one of the M replicas, which is also randomly selected. Then, an attempt was made to exchange their occupancy state,⁵² with a probability given by the Metropolis rule.⁵³ (ii) Replica exchange; this involves the exchange attempt of the X_i and X_j configurations, which correspond to the i th and j th adjacent replicas, which are randomly selected. The probability of exchange is given as follows:⁴⁹

$$W(X_i, T_i \rightarrow X_j, T_j) = \begin{cases} 1, & \text{if } \delta < 0 \\ \exp(-\delta) & \text{if } \delta \geq 0 \end{cases} \quad (2)$$

where $\delta = (1/k_B T_i - 1/k_B T_j)(H(X_j) - H(X_i))$ and k_B is the Boltzmann constant.

One tempering Monte Carlo step (TMCS) comprises repetition of steps (i) and (ii) $4L^2$ times.

The initialization of the M replicas starts with a random initial condition of the system. The final configuration of the first replica was obtained after n Monte Carlo steps (MCS) at T_1 (one MCS consists of L^2 realizations of the replica update sub-routine). Then, the initial configuration of the second replica was taken as the same as the final configuration of replica 1. In the same way, the initial configuration of the third replica was the same as the final configuration of the replica 2 (after n MCS at T_2) and so on for all replicas.³⁰ All the observables were averaged over each replica. Periodic boundary conditions were included in three spatial directions.

Moreover, 6×10^6 TMCS were needed to equilibrate each i replica. At low temperatures $T < T_c$, large quantities of TMCS were used to discard any possible metastable state. The quantities of the TMCS required for the parameters averaging step are the same as those needed in the equilibration step. Averages were taken over 5×10^2 different initial configurations. In all the cases, the standard statistical error bars are always smaller than the symbol size used in the figures. A total of $M = 50$ replicas were used, all equally spaced in each of the temperature ranges analyzed.

The simulations were carried out using a HUAUKE parallel cluster located at the Instituto de Bionanotecnología del NOA, Universidad Nacional de Santiago del Estero, Santiago del Estero, Argentina.

To study the phase transition by finite size scaling, it was necessary to properly define the thermodynamics parameters to be used. The geometrical order parameter will allow the recognition of the structural order of stage II from the disordered state. Stage II is characterized by two full insertion sites planes separated by an empty plane, as indicated in Fig. 1(b), where the red spheres are Li ions. In each plane, when $T < T_c$, Li ion forms a $(\sqrt{3} \times \sqrt{3})R30^\circ$ structure, as is shown in Fig. 1(c).

To describe stage II, a $(\sqrt{3} \times \sqrt{3})R30^\circ$ ordered structure, a global order parameter, ψ_p , was defined as follows:

$$\psi_p \equiv A|\rho_1 - \rho_2 + \rho_3 - \rho_4| \quad (3)$$

where $0.0 \leq \rho_i \leq 1.0$ is the local order parameter of the i plane, as indicated in Fig. 1(a) and $A = 1/2$ is the normalization constant. The $(\sqrt{3} \times \sqrt{3})R30^\circ$ structure has three different configurations with the same energy, each one situated in a different two-dimensional sub-lattice. This can be expressed as follows:

$$\rho_i \equiv b \sum_{j,k} |\theta_j - \theta_k| \quad (4)$$

where θ_j and θ_k are the surface coverage of the j and “ k ” sub-lattices, respectively. The sum of the differences was taken over the three sub-lattices. $b = 3/2$ is a normalization constant.

For stage II and $T < T_c$, $\psi_p = 1.0$; however, when $T > T_c$, the systems are completely disordered and $\psi_p \approx 0.0$.

The other quantities related are as follows: the susceptibility,

$$\chi(N, T) = N \frac{[\langle \psi_p^2 \rangle_T - \langle \psi_p \rangle_T^2]}{k_B T} \quad (5)$$

the energy per site,

$$E = \frac{\langle H \rangle}{N} \quad (6)$$

the specific heat, sampled from the energy fluctuations,

$$C_V(N, T) = \frac{[\langle H^2 \rangle_T - \langle H \rangle_T^2]}{Nk_B T^2} \quad (7)$$

and the reduced fourth-order cumulant⁵⁴

$$U_L(N, T) = 1 - \frac{\langle \psi_p^4 \rangle_T}{3(\langle \psi_p^2 \rangle_T)^2} \quad (8)$$

Another interesting quantity used to describe the system is the fourth-order cumulant of the energy. Using the energy per site E and its moments

$$U_{LE}(N, T) = 1 - \frac{\langle E^4 \rangle_T}{3(\langle E^2 \rangle_T)^2} \quad (9)$$

4. The order of the phase transition and estimation of the critical temperature

The full lithium-ion occupation in graphite (Li_xC_6 with $x = 1$) was equal to the third part of the total number of lattice sites. The lattice sizes used are as follows: $L = 12$ ($N = 576$), 18 ($N = 1296$), 24 ($N = 2304$), 30 ($N = 3600$), 36 ($N = 5184$), 42 ($N = 7056$), and 48 ($N = 9216$).

The order parameters, susceptibilities, specific heats, and energies per site are shown in Fig. 2(a–d) for different L sizes as a function of $k_B T$. The order parameters and the energy per site, (2a) and (2d), respectively, present a steep variation around the inflexion point, which is different for each size. The susceptibility and specific heat, (2b) and (2c), respectively, show a maximum value that increases with L . These maxima and inflection points coincide with the critical temperature for each size, $T_c(L)$. All these behaviors imply finite size effects, which indicate the existence of a phase transition.

To classify the order of the transition, it is convenient to analyze the Binder cumulants behaviour U_L and U_{LE} , defined in eqn (8) and (9), respectively. These parameters are shown in Fig. 3(a) and (b). As the lattice size increases, U_L presents a minimum whose value becomes more negative, and U_{LE} shows a peak that becomes sharper. In both cases, the trend followed by the cumulants corresponds to a first-order transition.^{27,30,38}

The critical temperature at the thermodynamic limit, $T_c(\infty)$, can be obtained *via* extrapolation of the $T_c(L)$ vs. V^{-1} plot for $U_{LE}(T)$, susceptibility, specific heat, and the logarithmic derivative of ψ_p . For these quantities, the next relationship can be written as follows:

$$T_c(L) = T_c(\infty) + aV^{-1}, \quad L \rightarrow \infty \quad (10)$$

where $V = 4L^2$ is the volume of the system and a is a constant that depends on the quantity considered, *i.e.* C_v , χ , ψ_p or U_{LE} .

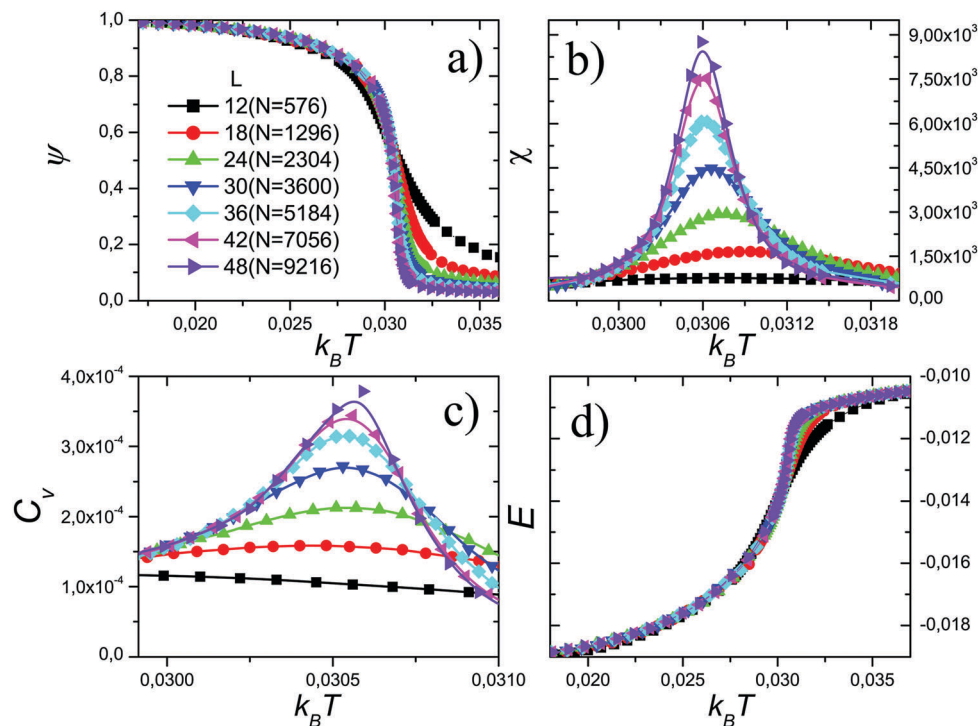


Fig. 2 Several thermodynamics parameters versus kT as a function of the size L : (a) The order parameter, (b) susceptibility (c) specific heat and (d) energy per site.

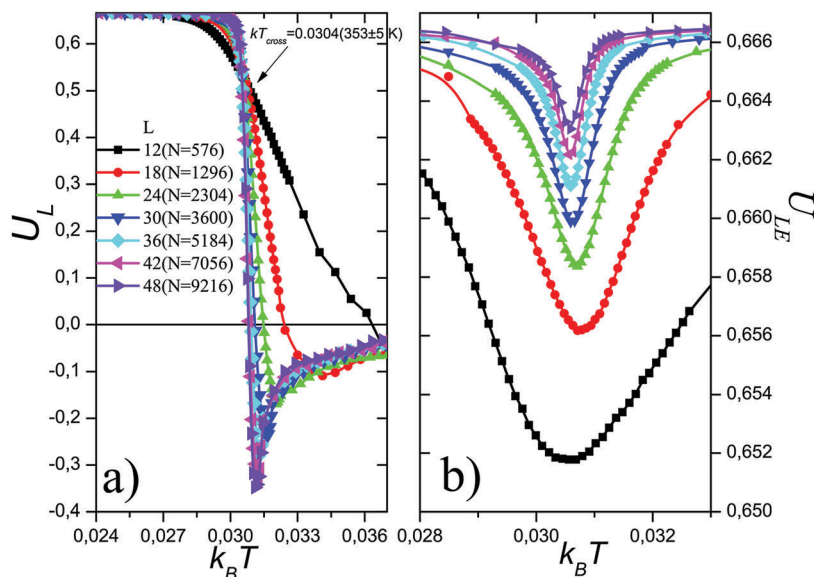


Fig. 3 (a) The fourth-order cumulant of the order parameter and (b) the fourth-order cumulant of energy.

This behavior is shown in Fig. 4, where it can be seen that $T_c(\infty) = 354.6 \pm 0.5$ K.

To confirm the order of the transition, the order parameters ($P(\psi_p)$) and energy per site ($P(E)$) distributions were analyzed. Both are in arbitrary units and were obtained for $L = 36$ at three different temperatures (Fig. 5). In both distributions, two peaks are observed in all the cases; several observations can be claimed: (i) At $T < T_c$ ($L = 36$), panels (a) and (d), the major

peak corresponds to the ordered phase, whereas the minor peak is the frequency of the disordered phase. (ii) At T_c ($L = 36$) = 355 ± 2 K, panels (b) and (e), the two peaks heights are practically equal, which means that both phases co-exist at the transition point. Finally, (iii) at $T > T_c$ ($L = 36$), the panels (c) and (f), the opposite of (i) takes place. All these observations are consistent with the behavior of a first-order phase transition.^{27,28}

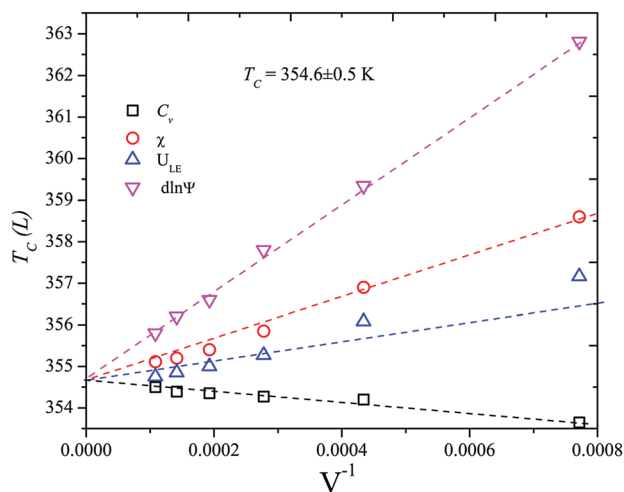


Fig. 4 $T_c(L)$ versus V^{-1} for C_v , χ , U_{LE} and $d \ln \psi$, as indicated.

Moreover, to complete the picture, it is possible to estimate the critical temperature as the temperature where the crossing of the U_L curves occurs (T_{cross}^{30} (Fig. 3(a)). Then, $T_{\text{cross}} = (353 \pm 5) \text{ K} \approx T_c$, this value was comparable with that obtained in the thermodynamic limit.

Although the phase transition seems to be a first-order transition, it is possible to establish power laws with the thermodynamic parameters, as shown Fig. 2, like in an order-disorder phase transition. Thus, following ref. 27, effective exponents can be obtained. It is important to notice that these exponents are not

critical. The way of measuring the effective exponents was similar to the method applied for the order-disorder phase transitions.^{55–59} From the standard theory of finite size scaling,^{15,38,50,60,61} the next relationship can be established as follows:

$$\begin{aligned} C_v &\propto L^{\frac{2\alpha}{\nu_e}}, \\ \psi_p &\propto L^{\frac{\beta_e}{\nu_e}}, \\ \chi &\propto L^{\frac{\gamma_e}{\nu_e}}. \end{aligned} \quad (11)$$

The sub-index e identifies the effective exponents. The next table summarizes all the effective exponents calculated in this study.

Effective exponent	Value
ν	1/2
β	1/5
γ	1/10
α	3/2

With these exponents, the Rushbrooke⁶² equality can be applied, which relates critical exponents as follows:

$$\frac{\alpha_e}{\nu_e} + \frac{2\beta_e}{\nu_e} + \frac{\gamma_e}{\nu_e} = \frac{2}{\nu_e} \quad (12)$$

In summary, from all the analyses performed herein, it is possible to observe that the behavior of the system in the

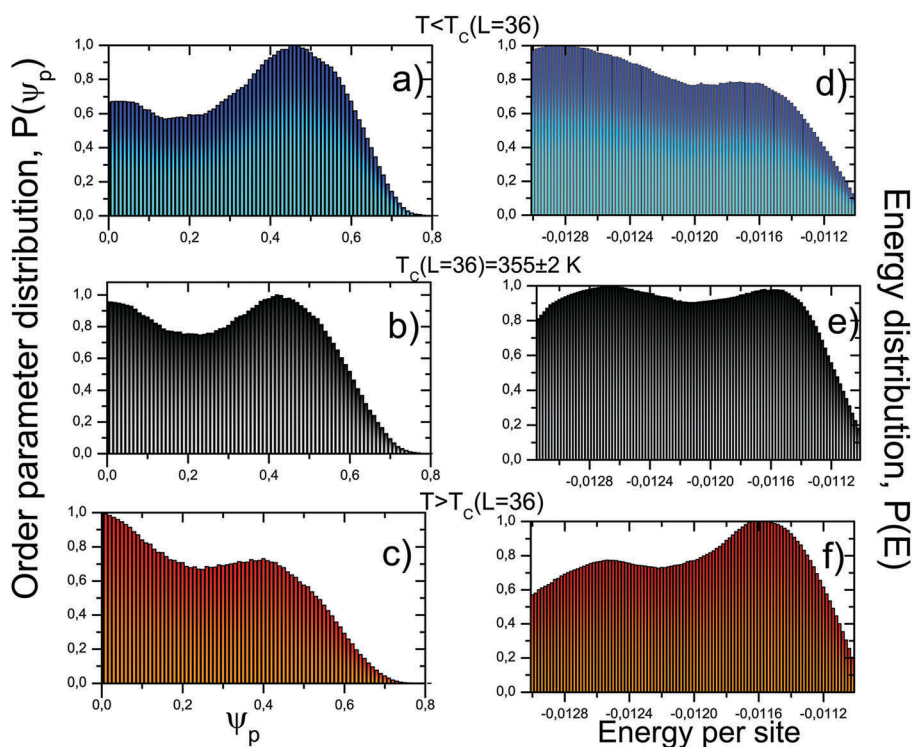


Fig. 5 The distributions for $T < T_c(L = 36)$, $T_c(L = 36) = 355 \pm 2 \text{ K}$ and $T > T_c(L = 36)$. The order parameter distribution $P(\psi_p)$: Panels (a–c). The energy per site $P(E)$ distribution: panels (e), (d) and (f).

critical region is similar to the development reported in ref. 28. Therefore, it is possible to identify this transition as a weak first-order phase transition. Otherwise, the effective exponents values determined herein are similar to those found *via* other MC studies on the discrete 3D, three-state Potts model (which yields a weak first-order phase transition).²⁹ This universality class was also observed in stage I by Landau theory.³⁷ The same results, for the α and β effective exponents, were obtained by Robinson *et al.*³⁵ in the experimental study of the melting transition of stage I.

5 Conclusions

Using the parallel tempering Monte Carlo technique in the canonical assembly, the criticality of the phase transition in stage II ($\text{Li}_{0.5}\text{C}_6$) was studied. In this study, a lattice gas-model for the graphite anode of a lithium-ion battery was implemented. The model comprised four planes with a triangular geometry, where Li ions could be intercalated. Moreover, two kinds of interactions were used: a Lennard-Jones potential, for particle interactions in the same plane, and a power law potential, for interactions between planes. The finite size scaling method was used to classify the order of the phase transition. The finite size effects observed in the parameters analyzed indicate that stage II was generated *via* a phase transition. The distribution of the order parameter and energy confirms the occurrence of a first-order phase transition at 354.6 ± 0.5 K. However, the parameters measured show a behavior similar to an order-disorder phase transition. All this evidence confirms that the occurrence of stage II can be identified as a weak first-order phase transition.

Conflicts of interest

There are no conflicts to declare.

Acknowledgements

The authors acknowledge the financial support received from CONICET PIP 11220130100547CO, PID CONICET 11220110100992, PID CONICET 11220150100624, Agencia Nacional de Promoción Científica Program BID-FONCyT PICT-2012-2324 and PICT-2015-1605, CICYT from National University of Santiago del Estero, and SeCyT from the National University of Cordoba. E. M. G. A. acknowledges the fellowship received from the CONICET.

References

- J. M. Tarascon, J. M. Tarascon, M. Armand and M. Armand, Issues and challenges facing rechargeable lithium batteries, *Nature*, 2001, **414**(6861), 359–367.
- Y. Hu and X. Sun, Flexible rechargeable lithium ion batteries: advances and challenges in materials and process technologies, *J. Mater. Chem. A*, 2014, **2**(28), 10712.
- A. Barré, B. Deguilhem, S. Grolleau, M. Gérard, F. Suard and D. Riu, A review on lithium-ion battery ageing mechanisms and estimations for automotive applications, *J. Power Sources*, 2013, **241**, 680–689.
- N. Nitta, F. Wu, J. T. Lee and G. Yushin, Li-ion battery materials: present and future, *Mater. Today*, 2015, **18**(5), 252–264.
- S. Goriparti, E. Miele, F. De Angelis, E. Di Fabrizio, R. Proietti Zaccaria and C. Capiglia, Review on recent progress of nanostructured anode materials for Li-ion batteries, *J. Power Sources*, 2014, **257**, 421–443.
- T. Ohzuku, Formation of Lithium-Graphite Intercalation Compounds in Nonaqueous Electrolytes and Their Application as a Negative Electrode for a Lithium Ion (Shuttlecock) Cell, *J. Electrochem. Soc.*, 1993, **140**(9), 2490.
- M. D. Levi and D. Aurbach, The mechanism of lithium intercalation in graphite film electrodes in aprotic media. Part 1. High resolution slow scan rate cyclic voltammetric studies and modeling, *J. Electroanal. Chem.*, 1997, **421**(96), 79–88.
- M. D. Levi, E. A. Levi and D. Aurbach, The mechanism of lithium intercalation in graphite film electrodes in aprotic media. Part 2. Potentiostatic intermittent titration and in situ XRD studies of the solid-state ionic diffusion, *J. Electroanal. Chem.*, 1997, **421**(96), 89–97.
- R. Yazami, PhD thesis, Grenoble University, France, 1985.
- D. Guerard and A. Herold, Intercalation of lithium into graphite and other carbons, *Carbon*, 1975, **13**(4), 337–345.
- S. B. DiCenzo, S. Basu and G. K. Wertheim, In-plane ordering in stage two lithium-graphite, *Synth. Met.*, 1981, **3**(1–2), 139–145.
- D. Billaud, F. X. Henry, M. Lelaurain and P. Willmann, Revisited structures of dense and dilute stage II lithium-graphite intercalation compounds, *J. Phys. Chem. Solids*, 1996, **57**(95), 775–781.
- K. Binder, Finite size effects on phase transitions, *Ferroelectrics*, 1987, **73**(1), 43–67.
- J. Cardy, *Finite-size Scaling*, Elsevier, vol. 2, 2012.
- V. Privman, *Finite-Size Scaling Theory, in Finite Size Scaling and Numerical Simulation of Statistical Systems*, ed. V. Privman, World Scientific Publishing Company, Singapore, 1990.
- K. Binder, Phase Transitions in Reduced Geometry, *Annu. Rev. Phys. Chem.*, 1992, **43**, 33–59.
- K. Binder, Finite size effects at phase transitions, *Computational Methods in Field Theory*, ed. C. B. Lang and A. Gausterer, Berlin, Heidelberg: Springer, 1992, pp. 59–125.
- K. Binder and H. Rauch, Numerische Berechnung von Spin-Korrelationsfunktionen und Magnetisierungskurven von Ferromagnetica, *Z. Phys.*, 1969, **219**(3), 201–215.
- K. Binder, Statistical mechanics of finite three-dimensional Ising models, *Physica*, 1972, **62**(4), 508–526.
- Y. Imry, Finite-size rounding of a first-order phase transition, *Phys. Rev. B: Condens. Matter Mater. Phys.*, 1980, **21**(5), 2042–2043.
- M. E. Fisher and A. N. Berker, Scaling for first-order phase transitions in thermodynamic and finite systems, *Phys. Rev. B: Condens. Matter Mater. Phys.*, 1982, **26**(5), 2507–2513.
- H. W. Blöte and M. Nightingale, Critical behaviour of the two-dimensional Potts model with a continuous number of

- states; a finite size scaling analysis, *Phys. A*, 1982, **112**(3), 405–465.
- 23 J. L. Cardy and P. Nightingale, Finite-size analysis of first-order phase transitions: Discrete and continuous symmetries, *Phys. Rev. B: Condens. Matter Mater. Phys.*, 1983, **27**(7), 4256–4260.
- 24 V. Privman and J. Rudnick, Nonsymmetric first-order transitions: Finite-size scaling and tests for infinite-range models, *J. Stat. Phys.*, 1990, **60**(5–6), 551–560.
- 25 K. Binder and D. Landau, Finite-size scaling at first-order phase transitions, *Phys. Rev. B: Condens. Matter Mater. Phys.*, 1984, **30**(3), 1477–1485.
- 26 M. E. Fisher and V. Privman, First-order transitions breaking $O(n)$ symmetry: Finite-size scaling, *Phys. Rev. B: Condens. Matter Mater. Phys.*, 1985, **32**, 447–464.
- 27 M. S. S. Challa, D. P. Landau and K. Binder, Finite-size effects at temperature-driven first-order transitions, *Phys. Rev. B: Condens. Matter Mater. Phys.*, 1986, **34**, 1841–1852.
- 28 K. Vollmayr and J. Reger, Finite size effects at thermally-driven first order phase transitions: A phenomenological theory of the order parameter distribution, *Z. Phys. B: Condens. Matter*, 1993, **125**, 113–125.
- 29 H. Herrmann, Monte Carlo simulation of the three-dimensional Potts model, *Z. Phys. B: Condens. Matter Quanta*, 1979, **35**(2), 171–175.
- 30 P. M. Pasinetti, F. Romá and A. J. Ramirez-Pastor, First-order phase transitions in repulsive rigid k-mers on two-dimensional lattices, *J. Chem. Phys.*, 2012, **136**(6), 0641131–0641138.
- 31 D. G. Onn, G. M. T. Foley and J. E. Fischer, Resistivity Anomalies and Phase Transitions in Alkali-metal Graphite Intercalation Compounds, *Mater. Sci. Eng.*, 1977, **31**, 271–275.
- 32 D. G. Onn, G. M. T. Foley and E. Fisher, Electronic properties, resistive anomalies, and phase transitions in the graphite intercalation compounds with K, Rb, and Cs, *Phys. Rev. B: Condens. Matter Mater. Phys.*, 1979, **19**(12), 6474–6483.
- 33 J. B. Hastings, W. D. Elleson and J. E. Fischer, Phase Transitions in Potassium-Intercalated Graphite: KC₂₄, *Phys. Rev. Lett.*, 1979, **42**(23), 1552–1556.
- 34 P. Bak and E. Domany, Order-disorder transitions in stage-2 graphite intercalation compounds, *Phys. Rev. B: Condens. Matter Mater. Phys.*, 1981, **23**(3), 1320–1324.
- 35 D. S. Robinson and M. B. Salomon, Universality, Tricriticality, and the Potts Transition in First-Stage Lithium-Intercalated Graphite, *Phys. Rev. Lett.*, 1982, **48**(3), 156–159.
- 36 J. Rossat-Mignod, A. Wiedenmann, K. C. Woo, J. W. Milliken and J. E. Fischer, First-order phase transition in the graphite compound LiC₆, *Solid State Commun.*, 1982, **44**(8), 1339–1342.
- 37 P. Bak and E. Domany, Theory of order-disorder transitions in the graphite intercalation compounds C₈Cs, C₈Rb, and C₆Li, *Phys. Rev. B: Condens. Matter Mater. Phys.*, 1979, **20**(7), 2818–2822.
- 38 O. A. Pinto, A. J. Ramirez-Pastor and F. Nieto, Phase diagrams for the adsorption of monomers with non-additive interactions, *Surf. Sci.*, 2016, **651**, 62–69.
- 39 E. M. Perassi and E. P. M. Leiva, A theoretical model to determine intercalation entropy and enthalpy: Application to lithium/graphite, *Electrochem. Commun.*, 2016, **65**, 48–52.
- 40 P. A. Derosa and P. B. Balbuena, A Lattice-Gas Model Study of Lithium Intercalation in Graphite, *J. Electrochem. Soc.*, 1999, **146**(10), 3630.
- 41 M. P. Mercer, S. Finnigan, D. Kramer, D. Richards and H. E. Hoster, The influence of point defects on the entropy profiles of Lithium Ion Battery cathodes: a lattice-gas Monte Carlo study, *Electrochim. Acta*, 2017, **241**, 141–152.
- 42 X. Zhang, T. T. Trinh, R. A. Van Santen and A. P. J. Jansen, Mechanism of the Initial Stage of Silicate Oligomerization, *J. Am. Chem. Soc.*, 2011, **133**(17), 6613–6625.
- 43 X. Zhang, A. Van Santen and A. P. J. Jansen, Kinetic Monte Carlo modeling of silicate oligomerization and early gelation, *Phys. Chem. Chem. Phys.*, 2012, **14**(34), 11969–11973.
- 44 H. M. Cuppen, L. J. Karssemeijer and T. Lamberts, The Kinetic Monte Carlo Method as a Way To Solve the Master Equation for Interstellar Grain Chemistry, *Chem. Rev.*, 2013, **113**(12), 8840–8871.
- 45 N. G. Almarza, J. Pkalski and A. Ciach, Periodic ordering of clusters and stripes in a two-dimensional lattice model. II. Results of Monte Carlo simulation, *J. Chem. Phys.*, 2014, **140**(16), 164708.
- 46 S. P. Kelty and C. M. Lieber, Atomic-resolution scanning-tunneling-microscopy investigations of alkali-metalgraphite intercalation compounds, *Phys. Rev. B: Condens. Matter Mater. Phys.*, 1989, **40**(8), 5856–5859.
- 47 J. C. Charlier, X. Gonze and J. P. Michenaud, First-Principles Study of the Stacking Effect on the Electronic Properties of Graphite (s), *Carbon*, 1994, **32**(2), 289–299.
- 48 Z. Y. Rong and P. Kuiper, Electronic Effects in Scanning-Tunneling-Microscopy – Moire Pattern on a Graphite Surface, *Phys. Rev. B: Condens. Matter Mater. Phys.*, 1993, **48**(23), 17427–17431.
- 49 K. Hukushima and K. Nemoto, Exchange Monte Carlo method and application to spin glass simulations, *J. Phys. Soc. Jpn.*, 1996, **65**, 1604–1608.
- 50 D. J. Earl and M. W. Deem, Parallel Tempering: Theory, Applications, and New Perspectives, *Phys. Chem. Chem. Phys.*, 2005, **7**(23), 3910–3916.
- 51 C. J. Geyer, *Markov Chain Monte Carlo Maximum Likelihood, 23rd Symposium on the Interface*, 1991, pp. 156–163.
- 52 K. Kawasaki, Diffusion Constant near the Critical point for Time-Dependent Ising Models. II, *Phys. Rev. Lett.*, 1966, **148**, 375–381.
- 53 N. Metropolis, A. W. Rosenbluth, M. N. Rosenbluth, A. H. Teller and E. Teller, Equation of state calculations by fast computing machines, *J. Chem. Phys.*, 1953, **21**(6), 1087–1092.
- 54 K. Binder, Finite size scaling analysis of ising model block distribution functions, *Z. Phys. B: Condens. Matter*, 1981, **43**, 119–140.
- 55 K. Binder, Surface Layer: a Simple Model for Magnetic Reconstruction, *Surf. Sci.*, 1985, **151**, 409–429.
- 56 A. M. Ferrenberg and D. P. Landau, Critical Behavior of the three-dimensional Ising model: A high-resolution Monte Carlo study, *Phys. Rev. B: Condens. Matter Mater. Phys.*, 1991, **44**(10), 5081–5091.

- 57 W. Janke, M. Katoot and R. Villanova, Single-Cluster Monte Carlo Study of the Ising Model on Two-Dimensional Random Lattices, *Phys. Rev. B: Condens. Matter Mater. Phys.*, 1994, **43**, 119.
- 58 K. Binder and E. Luijten, Monte Carlo tests of renormalization-group predictions for critical phenomena in Ising models, *Phys. Rep.*, 2001, **344**, 179–253.
- 59 F. Roma, J. L. Riccardo and A. J. Ramirez-Pastor, Critical behavior of repulsive dimers on square lattices at $2/3$ monolayer coverage, *Phys. Rev. B: Condens. Matter Mater. Phys.*, 2008, **77**, 195401.
- 60 P. M. Pasinetti, F. Romá, J. L. Riccardo and A. J. Ramirez-Pastor, Critical behavior of repulsive linear k -mers on triangular lattices, *Phys. Rev. B: Condens. Matter Mater. Phys.*, 2006, **74**(15), 1–8.
- 61 H. G. Katzgraber, K. Mathias and A. P. Young, Universality in three-dimensional Ising spin glasses: A Monte Carlo study, *Phys. Rev. B: Condens. Matter Mater. Phys.*, 2006, **73**, 224432.
- 62 G. S. Rushbrooke, On the Thermodynamics of the Critical Region for the Ising Problem, *J. Chem. Phys.*, 1963, **39**, 842.